THE JOURNAL OF BIOLOGICAL CHEMISTRY VOL. 289, NO. 22, pp. 15536–15543, May 30, 2014

Nitration Transforms a Sensitive Peroxiredoxin 2 into a More Active and Robust Peroxidase*

Received for publication, November 28, 2013, and in revised form, March 31, 2014 Published, JBC Papers in Press, April 9, 2014, DOI 10.1074/jbc.M113.539213

Lía M. Randall[‡§1], Bruno Manta[‡¶1,2], Martín Hugo[§||2], Magdalena Gil[‡‡], Carlos Batthyàny[§||**], Madia Trujillo[§||], Leslie B. Poole[§§], and Ana Denicola[‡§3]**

From the [‡]Laboratorio de Fisicoquímica Biológica, Instituto de Química Biológica, Facultad de Ciencias, Universidad de la República, 11400 Montevideo, Uruguay, the [§]Center for Free Radical and Biomedical Research, Facultad de Medicina, Universidad de la República, Montevideo 11100, Uruguay, the [¶]Laboratorio de Biología Redox de Tripanosomas, Institut Pasteur de Montevideo, 11400 Montevideo, Uruguay, the [||]Departamento de Bioquímica, Facultad de Medicina, Universidad de la República, 11100 Montevideo, Uruguay, the [**]Unidad de Bioquímica y Proteómica Analíticas, Institut Pasteur de Montevideo, 11400 Montevideo, Uruguay, the [‡‡]Unidad de Bioquímica y Proteómica Analíticas, Instituto de Investigaciones Biológicas Clemente Estable, Ministerio de Educación y Cultura, 11600 Montevideo, Uruguay, and the [§§]Department of Biochemistry, Wake Forest School of Medicine, Winston-Salem, North Carolina 27157

Background: Peroxiredoxin 2 (Prx2) reduces peroxides through a cysteine-dependent mechanism and is susceptible to overoxidation of its reactive cysteine during catalysis.
Results: Nitration rendered a more active peroxidase, less sensitive to overoxidation.
Conclusion: Nitration of Prx2 favors disulfide bond formation over overoxidation.
Significance: Understanding the mechanisms by which post-translational modifications modify Prx2 functionality *in vitro* is crucial to evaluate potential *in vivo* consequences for redox signaling.

Peroxiredoxins (Prx) are efficient thiol-dependent peroxidases and key players in the mechanism of H_2O_2-induced redox signaling. Any structural change that could affect their redox state, oligomeric structure, and/or interaction with other proteins could have a significant impact on the cascade of signaling events. Several post-translational modifications have been reported to modulate Prx activity. One of these, overoxidation of the peroxidatic cysteine to the sulfinic derivative, inactivates the enzyme and has been proposed as a mechanism of H_2O_2 accumulation in redox signaling (the floodgate hypothesis). Nitration of Prx has been reported *in vitro* as well as *in vivo*; in particular, nitrated Prx2 was identified in brains of Alzheimer disease patients. In this work we characterize Prx2 tyrosine nitration, a post-translational modification on a noncatalytic residue that increases its peroxidase activity and its resistance to overoxidation. Mass spectrometry analysis revealed that treatment of disulfide-oxidized Prx2 with excess peroxynitrite renders mainly mononitrated and dinitrated species. Tyrosine 193 of the YF motif at the C terminus, associated with the susceptibility toward overoxidation of eukaryotic Prx, was identified as nitrated and is most likely responsible for the protection of the peroxidatic cysteine against oxidative inactivation. Kinetic analyses suggest that tyrosine nitration facilitates the intermolecular disulfide formation, transforming a sensitive Prx into a robust one. Thus, tyrosine nitration appears as another mechanism to modulate these enzymes in the complex network of redox signaling.

Peroxiredoxins (Prx,[4] EC 1.11.1.15) are a group of enzymes that efficiently reduce peroxides based on a critical cysteine residue (peroxidatic cysteine, C_P). The first step in catalysis is the reaction of C_P with H_2O_2 to form a sulfenic acid derivative (C_P-SOH) which, in 2-cysteine Prx (2-Cys Prx), reacts with another cysteine residue (the resolving cysteine, C_R) to form a disulfide that is then reduced by the thioredoxin/thioredoxin reductase/NADPH system (Fig. 1) (1–4). In typical 2-Cys Prx or Prx1 subfamily (Prx 1–4 in mammals (5)), the reaction occurs between the C_P-SOH of one subunit with the C_R-SH of another subunit; thus, each homodimer contains two active sites (3). In addition, for the intermolecular disulfide to be formed, a conformational change is needed to approach the C_P-SOH from one subunit toward the C_R from the other subunit. This rearrangement involves the transition from the so-called fully folded (FF) form, in which the C_P and the C_R are approximately 14 Å apart, to a locally unfolded (LU) conformation (Fig. 1) (2, 7, 8).The sulfenic acid intermediate can react with the C_R-SH forming a disulfide, or with a second molecule of H_2O_2 to form sulfinic acid (overoxidation), inactivating the peroxidase activ-

* This work was supported, in whole or in part, by National Institutes of Health Grant GM050389 (to L. B. P.). This work was also supported by Comisión Sectorial de Investigación Científica UdelaR Grant CSIC C007-348 (to A. D.) and Agencia Nacional de Investigación e Innovación Grants FCE_2011_1_S706 (to M. T.) and FCE_2007_217 (to B. M.).
[1] Supported by Comisión Académica de Posgrados, UdelaR, and PEDECIBA (Programa de Desarrollo de las Ciencias Básicas).
[2] Supported in part by the Agencia Nacional de Investigación e Innovación.
[3] To whom correspondence should be addressed: Laboratorio de Fisicoquímica Biológica, Instituto de Química Biológica, Facultad de Ciencias, Universidad de la República, Iguá 4225, 11400, Montevideo, Uruguay. Tel./Fax: 598-2-525-0749; E-mail: denicola@fcien.edu.uy.

[4] The abbreviations used are: Prx, peroxiredoxin(s); C_P, peroxidatic cysteine; C_R, resolving cysteine; C_P-SOH, cysteine sulfenic acid; C_P-SO_2H, cysteine sulfinic acid; DTDP, 4′,4′-dithiodipyridine; DTNB, 5′,5′-dithio-bis(2-nitrobenzoic acid); DTPA, diethylenetriaminepentaacetic acid; ESI, electrospray ionization; FF, fully folded; LU, locally unfolded; NEM, *N*-ethylmaleimide; Prx2, peroxiredoxin 2; PTM, post-translational modification; QTOF, quadrupole time-of-flight; ROA, reverse-order addition; TR, thioredoxin reductase; Trx, thioredoxin.

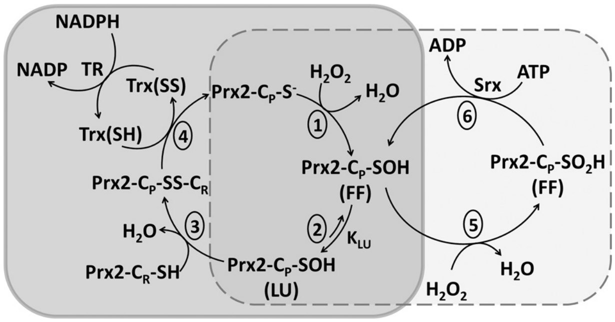

FIGURE 1. **Catalytic cycle of eukaryotic typical 2-Cys Prx.** *1*, reaction of a molecule of peroxide with the C_P thiolate to form cysteine sulfenic acid. *2*, transition from the FF to the LU conformation. *3*, reaction of C_P sulfenic acid with C_R. *4*, reduction of disulfide Prx. *5*, overoxidation of C_P to sulfinic acid. *6*, reduction of cysteine sulfinic acid by sulfiredoxin (*Srx*)/ATP. The protein is represented as one of two active sites within a functional dimer.

ity. The oxidation of cysteine to cysteine sulfinic acid (C_P-SO_2H) is an irreversible post-translational modification (PTM) for most proteins other than 2-Cys Prx, where the specific enzymatic reduction of C_P-SO_2H by sulfiredoxin in an ATP-dependent mechanism was demonstrated (9, 10).

Prx are ubiquitous and highly expressed proteins, and their extraordinary reactivity and specificity for hydroperoxides make them ideal sensors of endogenous H_2O_2 and probably the first step in H_2O_2-induced signaling pathways (11–15). PTM of Prx that could affect their activity, redox state, oligomeric structure, or interaction with other proteins will undoubtedly affect redox signaling by H_2O_2, and it has been hypothesized that Prx inactivation via overoxidation is a way to accumulate H_2O_2 to allow oxidation of other redox proteins (the floodgate hypothesis) (2). The presence of sulfiredoxin as an enzyme that specifically reduces typical 2-Cys Prx cysteine sulfinic acid supports the biological relevance of their peroxidase activity and the signaling role of their oxidative inactivation (16).

Prx2, the most abundant peroxidase in mammalian erythrocytes (17, 18), is capable of reducing hydroperoxides as well as peroxynitrite,[5] a potent oxidant formed *in vivo* by the diffusion-controlled reaction between superoxide and nitric oxide. Our group recently demonstrated that erythrocyte Prx2 not only is susceptible to overoxidation by peroxynitrite, but it can also get nitrated during catalysis (19). Moreover, nitrated Prx2 was detected in brains of patients with early Alzheimer disease (20).

Protein tyrosine nitration is a common PTM occurring under conditions of nitroxidative stress, which alters the structure and function of the modified protein. The biological mechanism of tyrosine oxidation begins with the formation of the tyrosyl radical followed by addition of nitrogen dioxide yielding 3-nitrotyrosine, and one of the major pathways of protein nitration *in vivo* involves the reaction of radicals derived from peroxynitrite homolysis (21–25).

We herein report the effects of Prx2 modification by peroxynitrite treatment, focusing on tyrosine nitration, which increases its peroxidase activity along with resistance to overoxidation by H_2O_2. We hypothesize that nitration of tyrosine 193 from the YF motif at the C terminus, close to the active site, favors transition from the FF to the LU conformation, promoting disulfide formation and inhibiting C_P overoxidation.

EXPERIMENTAL PROCEDURES

Chemicals—Dithiothreitol (DTT), DTNB, and reduced nicotinamide adenine dinucleotide phosphate (NADPH) were purchased from AppliChem (Germany). DTDP was purchased from ACROS Organics, Fisher Scientific. Hydrogen peroxide (H_2O_2) and DTPA were purchased from Sigma. Peroxynitrite was synthesized as in Ref. 26. All other reagents were of analytical grade and used as received.

Purification of Proteins—Human Prx2 was purified from human erythrocytes according to Ref. 19. Recombinant human thioredoxin (hTrx1), *Escherichia coli* thioredoxin 1 (*Ec*Trx1), and recombinant *E. coli* thioredoxin reductase (*Ec*TR) were produced and purified as reported in Refs. 19 and 27. *Ecchinococcus granulosus* (*Eg*TR) was kindly provided by Dr. G. Salinas (28).

Peroxide and Protein Quantification—The concentration of H_2O_2 stock solutions was measured at 240 nm ($\epsilon_{240} = 43.6\ \text{M}^{-1}\ \text{cm}^{-1}$). Peroxynitrite concentration was determined at 302 nm ($\epsilon_{302} = 1670\ \text{M}^{-1}\ \text{cm}^{-1}$) as in Ref. 26. Protein concentration was measured by absorption at 280 nm in the assay buffer, using the corresponding ϵ determined for the oxidized proteins according to Ref. 29: ϵ_{280}(Prx2) = 19,380 $\text{M}^{-1}\ \text{cm}^{-1}$, ϵ_{280}(hTrx) = 7100 $\text{M}^{-1}\ \text{cm}^{-1}$, ϵ_{280}(*Ec*Trx) = 14,060 $\text{M}^{-1}\ \text{cm}^{-1}$, and ϵ_{280}(*Ec*TR) = 19,160 $\text{M}^{-1}\ \text{cm}^{-1}$. Concentration of active *Eg*TR was estimated according to FAD and selenium content (28).

Thiol Quantification—The thiol concentration of the reduced proteins was measured according to Ref. 30 with minor modifications. Briefly, the protein was reduced with DTT (>10-fold molar excess for 30 min) and the remnant reductant removed by buffer exchange with a HiTrap coupled to a FPLC with online UV detection equilibrated in 50 mM potassium phosphate buffer, pH 7.4, with 0.1 mM DTPA and 150 mM NaCl. An excess of DTDP was added to the protein sample in the assay buffer, and absorption was measured at 324 nm (ϵ_{324} = 21,400 $\text{M}^{-1}\ \text{cm}^{-1}$).

Prx2 Thiol Reduction and Oxidation—For reduction of purified Prx2, the enzyme was reduced with 1 mM DTT for 30 min at room temperature immediately before the experiment, and the mixture was passed twice through a Bio-Spin column (Bio-Rad) preequilibrated with the assay buffer. Thiol concentration was determined just after elution from the column, and controlled oxidation to its disulfide form was achieved with the addition of 0.6 eq of H_2O_2.

Nitration of Prx2 by Peroxynitrite—To prevent overoxidation of C_P, treatment with peroxynitrite was performed on the disulfide-oxidized enzyme. The corresponding molar excess of peroxynitrite was added in a unique bolus or a flux-like addition. Previously decomposed peroxynitrite in the assay buffer (reverse-order addition (ROA)) was used as a control of peroxynitrite-derived products reaction with Prx2. Tyrosine nitration of Prx2 was confirmed by Western blot analysis using specific antibodies. Briefly, samples were prepared for 15% SDS-PAGE under reducing (Figs. 2*B* and 4*C*) or nonreducing conditions (Fig. 3) without heating and transferred to a PVDF membrane. The membrane was incubated with anti-nitroty-

[5] The term peroxynitrite is used to refer to the sum of peroxynitrite anion ($ONOO^-$) and peroxynitrous acid (ONOOH) unless specified.

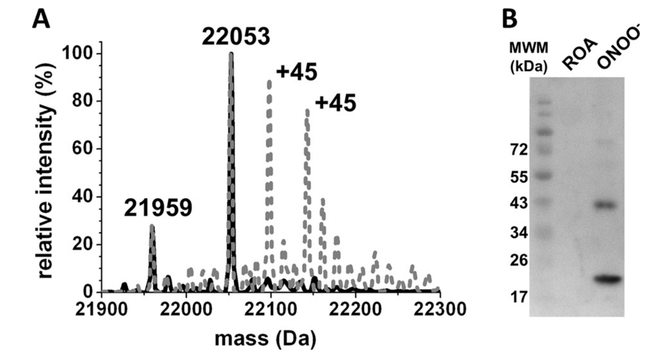

FIGURE 2. **Analysis of Prx2 nitration after peroxynitrite treatment.** *A*, QTOF-ESI MS analysis. Disulfide-oxidized Prx2 was treated with a 5-fold excess peroxynitrite, then reduced with 5 mM DTT for 15 min at room temperature, followed by addition of 20 mM NEM to block the reduced thiols. The remaining DTT and NEM were removed by gel filtration, and samples in 30 mM ammonium bicarbonate buffer were analyzed by QTOF-ESI MS. Control Prx2 is shown in *black* (shown as 100%), and the *gray dotted line* shows the peroxynitrite-treated enzyme. *B*, Western blot analysis. Disulfide Prx2 was treated with a 5-fold excess peroxynitrite ($ONOO^-$) or ROA. 2.4 μg of control or peroxynitrite-treated Prx2 was resolved on 15% SDS-PAGE under reducing conditions and analyzed by Western blot using α-NO_2Y antibodies.

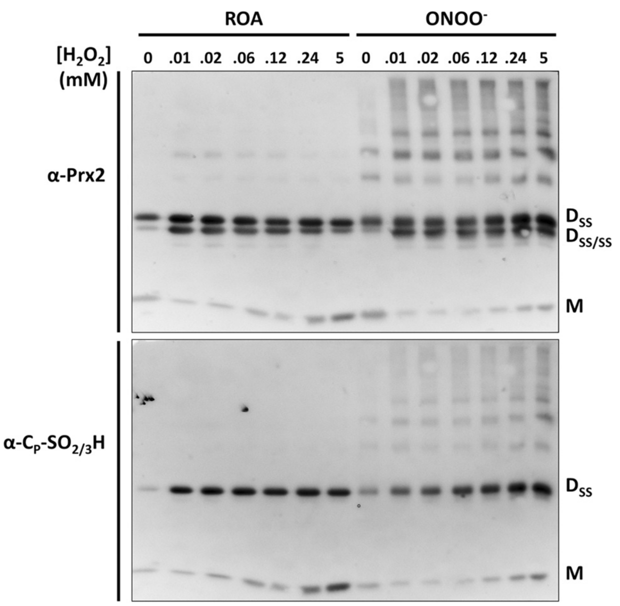

FIGURE 3. **Differential overoxidation of control and peroxynitrite-treated Prx2.** After treatment with the ROA control or a 5-fold excess of peroxynitrite ($ONOO^-$), Prx2 was treated with DTT for reduction of its thiols, and residual DTT was removed. 5 μM Prx2 was incubated with 0, 0.01, 0.02, 0.06, 0.12, 0.24, or 5 mM H_2O_2 in 50 mM phosphate buffer, pH 7.4. After 5 min, 30 mM NEM was added to alkylate the remaining thiols. Samples were prepared for SDS-PAGE under nonreducing conditions, analyzed by Western blotting using α-Prx2 antibody and α-C_P-$SO_{2/3}$H after mild stripping. One μg of protein was loaded on each *lane* (*D_{ss}*, dimer with one C_P disulfide-oxidized; *$D_{ss/ss}$*SS/SS, dimer with both C_P disulfide-oxidized; *M*, monomer).

rosine antibodies (α-NO_2Y (31)) in a 1/1000 dilution and with goat anti-rabbit IRDye® 800 CW (LI-COR Biosciences) secondary antibody (1/20,000).

Overoxidation of Prx2 by H_2O_2—To study the effect of nitration on the susceptibility of Prx2 to overoxidation, it was necessary to start with a reduced nonoveroxidized but yet nitrated form of Prx2. Disulfide-oxidized Prx2 was treated with peroxynitrite for nitration as described above, then reduced, and after removal of residual DTT the enzyme was treated with H_2O_2. Samples were resolved in 15% SDS-PAGE under nonreducing conditions, transferred to a PVDF membrane, and blotted with specific α-Prx2-C_P-$SO_{2/3}$H antibodies (AbFrontier). For control, rabbit polyclonal antibodies against Prx2 were used (α-Prx2; AbFrontier).

Mild Stripping of Western Blot Membranes—Membranes were incubated for 10-min in mild stripping buffer (1.5% glycine, 0.1% SDS, pH 2.2) twice, followed by two 10-min incubations in PBS and two 5-min incubations in TBS-Tween 0.1%. Blockage was performed for 2 h or overnight in 5% milk in TBS-Tween 0.1%.

NADPH-linked Peroxidase Activity—NADPH consumption was followed spectrophotometrically at 340 nm in a Cary 50 spectrophotometer (Varian). Prx2 was mixed with 120 μM NADPH, 0.4 μM *Eg*TR, 8 μM hTrx1 in the described buffer, and the reaction was started with the addition of H_2O_2. An Applied Photophysics RX2000 Rapid Kinetics Spectrophotometer Accessory was used for stopped-flow experiments.

Thioredoxin-linked Peroxidase Activity—The catalytic H_2O_2 decomposition by Prx2 was followed through the intrinsic fluorescence (λ_{exc} = 280 nm, λ_{em} = 340 nm) of reduced *Ec*Trx1 (10 μM) in a coupled assay with Prx2 (50 nM) and H_2O_2 (7 μM) in a thermostatted Cary Eclipse spectrofluorometer (Varian). Fluorescence changes were calibrated using a known concentration of reduced and oxidized *Ec*Trx1.

MS Analysis of Prx2 Tryptic Digestion—For analysis of proteins obtained from acrylamide gels, selected bands were manually cut and in-gel digested with trypsin (sequence grade; Promega) as described (32). Peptides were extracted from gels using aqueous 60% acetonitrile containing 0.1% TFA and concentrated by vacuum drying. Mass spectra of peptides mixtures were acquired in a linear ion trap mass spectrometer (LTQ Velos, Thermo) coupled on-line with a nano-liquid chromatography system (easy-nLC; Proxeon-Thermo). Peptides were separated in a reversed-phase column (EASY-column™ C18, 75 μm × 10 cm, inner diameter) equipped with a trap column (EASY-column C18, 100 μm × 2 cm, inner diameter) with solvent A (0.1% formic acid in H_2O) and solvent B (0.1% formic acid in acetonitrile), and eluted using a linear gradient from 0 to 45% B in 70 min at 300 nl/min. Electrospray voltage was 1.6 kV, capillary temperature was 270 °C. Peptides detected in the positive ion mode using a mass range of 300–2000.

Proteins were identified by database searching of measured peptide m/z values using the MASCOT search engine (Matrix Science) and Sequest (Thermo) software, based on the following search parameters: monoisotopic mass tolerance, 1.5 Da; fragment mass tolerance, 0.8 Da; partial methionine oxidation, cysteine carbamidomethylation, tyrosine nitration, and three missed tryptic cleavages allowed. Protein mass and taxonomy were unrestricted. Significant scores ($p < 0.05$) were used as criteria for positive peptide identification.

Whole Protein Mass Spectrometry Analysis of Peroxynitrite-treated Prx2—Control and peroxynitrite-treated Prx2 were reduced, and 20 mM NEM was added to alkylate thiols. Remaining DTT and NEM were removed using Bio-Gel P6 Gel® (Bio-Rad) columns and 30 mM ammonium bicarbonate buffer for elution. Samples were diluted from 4 to 40 μl with methanol: H_2O 1:1 2% formic acid, and 2–3 μl were analyzed using a Waters Q-Tof API US operated in "V" mode using a Triversa

Nanomate sprayer from Advion. Sprayer voltage ~ 1.8 kV; Q-T of cone voltage 45 V; source temperature 80 °C; nitrogen desolvation temperature 200 °C. Data were acquired from 600–1900 m/z in positive ion continuum mode; scan time 2.4 s; interscan delay 0.1 s. Max Ent data were produced for 10,000–50,000 Da.

RESULTS

Treatment of Prx2 with Peroxynitrite Yields a Nitrated Enzyme—Disulfide-oxidized Prx2 was treated with a 5-fold excess of peroxynitrite or its decomposition products, as a control designated ROA. Nitration of Prx2 was confirmed by inmunoblotting and mass spectrometry analyses (Fig. 2). For QTOF-ESI mass spectrometry analysis, disulfide-oxidized Prx2 was reduced with DTT and alkylated with NEM. A main peak of m/z 22,053 was obtained for control Prx2, which corresponds to the Prx monomer (21,803 Da) with both C_P and C_R alkylated with NEM (125 Da) (Fig. 2*A*). When treated with a 5-fold excess of peroxynitrite, mainly mononitrated (m/z 22,053 ± 45) and dinitrated (m/z 22,053 ± (2 × 45)) species were detected, confirming that nitration is the main modification after peroxynitrite treatment of disulfide Prx2. The minor species detected in both experiments (m/z 21,959) corresponds to the monomer of Prx2 with one Cys NEM-alkylated and the other one overoxidized, suggesting initial oxidation of Prx2 with H_2O_2 to obtain the disulfide form rendered a minor portion of overoxidized protein (Fig. 2*A*). Western blot analysis using antibodies against nitrotyrosine residues confirmed tyrosine nitration after the peroxynitrite treatment (Fig. 2*B*). Some nonreducible dimers were observed, suggesting the presence of di-tyrosine dimers, characteristic of peroxynitrite treatment of proteins (22).

Analysis of Peroxynitrite-treated Prx2 Overoxidation—2-Cys Prx sensitivity to overoxidation can be followed by nonreducing SDS-PAGE (33, 34). As shown in Fig. 3, and consistent with results in Fig. 2, overoxidation was detected at lower H_2O_2 concentrations for the nontreated Prx2 than for the peroxynitrite-treated enzyme. Addition of increasing concentrations of H_2O_2 to reduced control or peroxynitrite-treated Prx2 caused the transition from reduced monomer (M) to mono-disulfide dimer (D_{SS}) and di-disulfide dimer ($D_{SS/SS}$), with high H_2O_2 concentrations rendering overoxidized disulfide dimer (D_{SS}) and overoxidized monomer (M). As observed previously (33, 35), substoichiometric addition of H_2O_2 was enough to overoxidize the enzyme in these conditions, leading to the formation of dimers containing a disulfide and an overoxidized C_P, whereas high concentrations of the oxidant were not able to completely overoxidize the enzyme to its monomers. This result supports the idea of asymmetry of the homodimer active sites, suggesting that, under noncatalytic conditions, the redox state of one C_P affects overoxidation of the second one, as discussed previously by others (35–38). Moreover, nitration protected Prx2 from overoxidation, as the treated enzyme showed less overoxidation after H_2O_2 treatment than the control under noncatalytic conditions, suggesting a structural connection between tyrosine nitration and overoxidation of the peroxidatic cysteine.

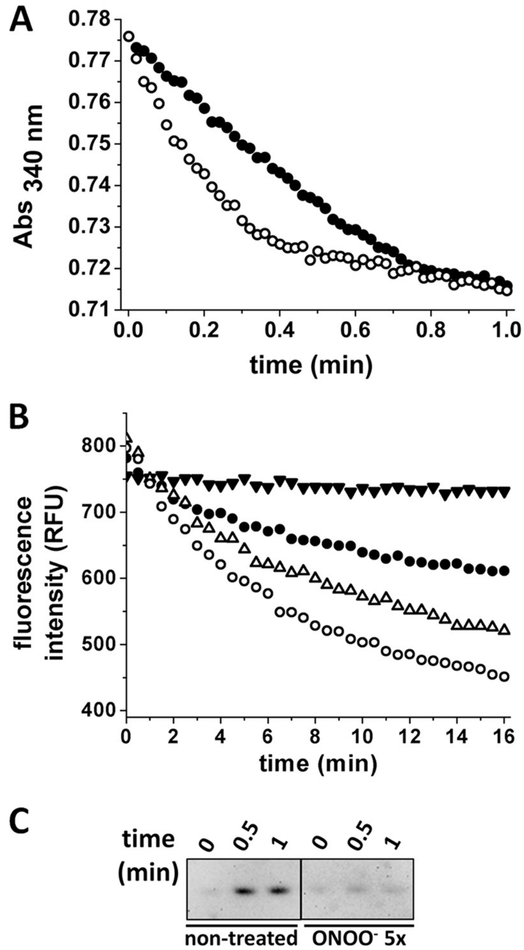

FIGURE 4. **Effect of nitration on Prx2 peroxidase activity and overoxidation.** *A*, NADPH-linked peroxidase activity. 0.5 μM reverse-order addition (●) or peroxynitrite-treated (○) Prx2 was incubated with 8 μM hTrx1, 0.4 μM *Eg*TR, and 160 μM NADPH in 50 mM sodium phosphate buffer, pH 7.4, 150 mM NaCl, 0.l mM DTPA. The reaction was started by the addition of H_2O_2 (10 μM final concentration), and consumption of NADPH was followed at 340 nm. *B*, *Ec*Trx1 fluorescence-linked Prx2 peroxidase activity. Oxidation of *Ec*Trx1 was followed at λ_{exc} = 280 nm, λ_{em} = 340 nm, in 50 mM sodium phosphate buffer, pH 7.4, 0.1 mM DTPA, 150 mM NaCl, with 10 μM reduced *Ec*Trx1. and 50 nM Prx2. ●, nontreated Prx2; △, Prx2 treated with 1-fold or (○) 5-fold excess peroxynitrite; ▼, control run (no Prx2 added). The reaction was started by the addition of 7 μM H_2O_2. *C*, Western blot analysis against C_P-$SO_{2/3}H$. Aliquots were taken at 0, 0.5, and 1 min after H_2O_2 addition in the presence of Trx, TR, and NADPH. Catalase (0.3 mg/ml) was added to eliminate residual H_2O_2 and NEM (26 mM) to block remaining thiols. 80 ng of Prx2 was loaded on each *lane* and resolved by reducing SDS-PAGE.

Treatment of Prx2 with Peroxynitrite Affects Its Peroxidase Activity—Peroxidase activity was measured following the consumption of NADPH at 340 nm after addition of H_2O_2 to a system containing Prx2, hTrx1, *Eg*TR, and NADPH (Fig. 4*A*). Treated Prx2 showed a higher rate of H_2O_2 reduction than the ROA control. The gain in peroxidase activity was confirmed by following NADPH consumption in a stopped-flow spectrophotometer, demonstrating that the change in peroxidase activity precedes oxidative inactivation of the enzyme (data not shown), as well as following the loss of reduced *Ec*Trx1 fluorescence at 340 nm (λ_{exc} = 280 nm) as it was oxidized by Prx2/H_2O_2 (Fig. 4*B*). The inactivation during turnover was clear for the native Prx2, whereas the peroxynitrite-treated enzyme suffered less overoxidation in turnover, as indicated by Western blot analysis (Fig. 4*C*).

Interaction of Nitrated Prx2 with hTrx1 Does Not Explain the Increase in Peroxidase Activity—To understand the gain in Prx2 peroxidase activity after treatment with peroxynitrite, we measured peroxidase activity using increasing concentrations of hTrx1 at a fixed concentration of H_2O_2 (Fig. 5). Interestingly, when low concentrations of hTrx1 were used, control and treated-Prx2 showed no clear differences in their peroxidase activity, whereas increasing hTrx1 concentrations enhanced their differences. As shown in Fig. 5, even in the presence of high concentrations of hTrx1 (>10-fold the reported K_m^{app} (19)), a significant difference between untreated and peroxynitrite-treated Prx2 activity was observed. Fitting the data from Fig. 5 to the Michaelis-Menten equation, V_{max} can be calculated, obtaining a higher value for the peroxynitrite-treated enzyme than for control Prx2.

Mapping of the Modified Residues Reveals Nitration of Tyr-193—Analysis of digested Prx2 in an LTQ mass spectrometer mapped four of the seven tyrosine residues of the polypeptidic chain. From these peptides, three of the residues (Tyr-33, Tyr-126, and Tyr-193) were detected as nitro-tyrosines after peroxynitrite treatment, whereas Tyr-115 was found as native in every experiment. Table 1 shows the theoretical and experimental mass values for the modified tyrosine-containing peptides detected. Among these, Tyr-193 is part of the YF motif located in the C terminus region of the protein that has been related to Prx sensitivity to overoxidation (Fig. 6) (2), and the environment of the YF loop has been recently described to have a great impact on C_P overoxidation (35).

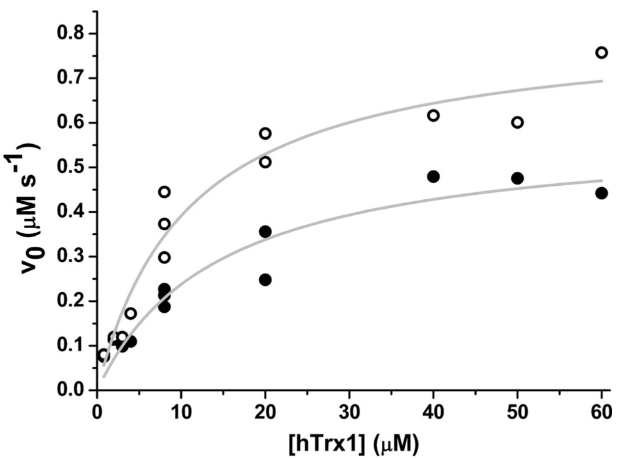

FIGURE 5. **Dependence of Prx2 peroxidase activity with thioredoxin concentration.** Nontreated (●) or 5-fold excess peroxynitrite-treated (○) Prx2 activity was measured following NADPH consumption at 340 nm. The reaction was started with the addition of 10 μM H_2O_2 to a mixture containing 160 μM NADPH, 0.4 μM *Eg*TR, varying concentrations of hTrx1 (0.8–60 μM), and 0.5 μM Prx2.

DISCUSSION

The peroxidatic cysteine of Prx reacts with H_2O_2 at 10^3- to 10^6-fold faster than most protein cysteines (13), but at ordinary rates with any other thiol reagent (39). Prx seem to be designed to specifically reduce peroxides, which place them not only as efficient antioxidant enzymes but also as key players in the mechanism of H_2O_2-induced redox signaling (40, 41). The catalysis of H_2O_2 reduction depends on a conserved Cys residue within a highly conserved active site pocket that adequately stabilizes the transition state. In addition, an important conformational change is needed for 2-Cys Prx to complete the oxidative part of the cycle, including the local unfolding of the helix that harbors C_P and the displacement of secondary structure elements that contain the C_R residue (2). Stabilization of the FF form of the enzyme has been associated with a slower rate of disulfide formation favoring the reaction of C_P-SOH with H_2O_2 to form the inactive sulfinic derivative (C_P-SO_2H). This inactivation by overoxidation has been postulated as a mechanism of regulating intracellular H_2O_2 levels, critical for redox signaling (2, 14, 42–44).

MS analysis of disulfide Prx2 treated with a 5-fold excess of peroxynitrite revealed that the main polypeptidic modification was nitration of tyrosine residues yielding mainly mononitrated and dinitrated species (Fig. 2*A*). Nitration of Prx2 rendered an enzyme less susceptible to overoxidation by H_2O_2 (Figs. 3 and 4*C*). This could be due either to a slower reaction with the second H_2O_2 molecule to yield the sulfinic derivative (step 5 in Fig. 1) or to a faster formation of the intermolecular disulfide (steps 2 and 3 in Fig. 1), thus unfavoring the overoxidation reaction.

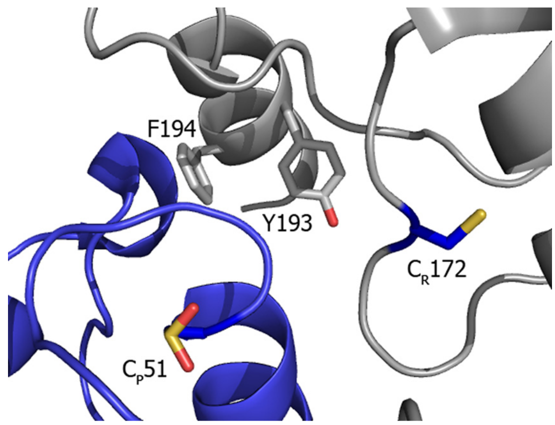

FIGURE 6. **Structural model of Prx2 active site.** View of human erythrocyte Prx2 active site. One monomer shows the C_P residue in sulfinic acid form (*blue*) whereas the other subunit (*gray*) shows the C_R, as well as the YF motif containing Tyr-193. The image was constructed with PyMOL from PDB 1QMV (6).

TABLE 1

Identification of modified tyrosine-containing peptides after treatment with peroxynitrite

Control and peroxynitrite-treated Prx2 were digested with trypsin after 15% SDS-PAGE. Samples were subjected to HPLC-MS/MS using an LTQ mass spectrometer as detailed under "Experimental Procedures." Sequences of modified tyrosine-containing peptides identified by MS are shown, with their corresponding theoretical and observed masses.

Peptide	Theoretical mass [(M + H)+]	Theoretical mass + 45[a] [(M + H)+]	Observed masses	Assigned sequence	Nitrated tyrosine
	Da	*Da*	*Da*		
1	625.3	670.3	670.2	^{30}LSD^{33}YK^{34}	Tyr-33
2	673.3	718.3	718.2	^{192}E^{193}YFSK^{196}	Tyr-193
3	924.4	969.4	969.3	^{120}TDEGIA^{126}YR^{127}	Tyr-126

[a] Addition of a nitro ($-NO_2$) group results in a molecular mass increase of 45 Da.

Surprisingly, the peroxynitrite-treated enzyme was more active than the native enzyme (Fig. 4). Given the modified enzyme is more resistant to overoxidation, one possible explanation for the observed gain in activity could be less inactivation in turnover (as seen in Fig. 4*C*). However, measurement of activity by stopped-flow spectrophotometry showed a higher rate for the nitrated enzyme from the very beginning of the run (0.277 ± 0.006 μmol/min *versus* 0.213 ± 0.002 μmol/min for the untreated enzyme; data not shown), indicating the differences in activity preceded overoxidation in turnover.

The reaction of C_P with H_2O_2, the first step in catalysis, is so fast ($k_2 = 10^7$–10^8 M^{-1} s^{-1}) that it is safe to assume C_P-SOH formation will not be the limiting step (19, 39). Thus, under the experimental conditions employed, the gain in peroxidase activity should reside in disulfide formation between C_P-SOH and C_R and/or the reduction of the intermolecular disulfide by thioredoxin (Fig. 1). The first option will be kinetically limited by the conformational change needed to get together both cysteines (the FF-LU transition (8)) whereas the second is limited by the kinetics of protein-protein interaction (Fig. 1). As shown in Fig. 5, at a fixed saturating concentration of H_2O_2, initial NADPH consumption rates were very close for control and peroxynitrite-treated Prx2 at low concentrations of hTrx1, whereas a significant difference appeared at higher hTrx1 concentrations. Although a faster dissociation of the ternary complex between hTrx1 and Prx2 to yield reduced Prx2 could explain the observed differences in V_{max}, it cannot explain the resistance to overoxidation of the nitrated enzyme. Therefore, it can be affirmed that, at high hTrx1 concentrations, the velocity of NADPH consumption is limited by disulfide formation. From V_{max} and Prx2 concentration, the rate constant of this step, k_{cat}, can be estimated, obtaining a value of (1.2 ± 0.1) s^{-1} for the ROA control enzyme and (1.6 ± 0.1) s^{-1} for the peroxynitrite-treated Prx2. Very similar results were obtained when using *Ec*TR and *Ec*Trx1 (data not shown), supporting the idea that the observed changes in V_{max} are not due to differences in the interaction between Prx2 and Trx. The faster the intermolecular disulfide bond is formed, the lower the chance for C_P to get overoxidized by H_2O_2. These differences in k_{cat} explain the differences in activity as well as the different susceptibility to overoxidation. Thus, this PTM transforms a sensitive Prx into a more robust peroxidase.

It has been observed that eukaryotic Prx, generally more sensitive to overoxidation than prokaryotic Prx, present a YF motif at the C terminus (Fig. 6) that packs over the active site in the FF form of the protein and delays the conformational change that brings together C_P and C_R, therefore slowing down the disulfide formation and favoring the overoxidation reaction (3, 8, 33, 35). In addition, different susceptibility toward overoxidation was found between different mammalian 2-Cys Prx isoforms. Human mitochondrial Prx3 is more resistant to this modification than cytosolic Prx2 (33). Recent work by Haynes *et al.* (35). demonstrated that residues near the C_R at the C terminus modulate the extent of C_P overoxidation. The substitution of residues at the C terminus of Prx3 resulted in a Prx2-like enzyme, more susceptible to overoxidation (35). Moreover, truncation of the C terminus containing the YF motif was reported to decrease overoxidation of Prx (45, 46). The YF sequence motif in the C-terminal helix of one subunit covers helix α2 containing the C_P of the adjacent subunit, stabilizing the FF form, thus making difficult the unfolding of the C_P-containing α2 to reach C_R (2). Tyr-193, which was nitrated by peroxynitrite treatment (Table 1) belongs to this YF motif and is most likely responsible for the resistance to overoxidation of the nitrated enzyme (Fig. 6). It is interesting to note that in *in vitro* experiments where Jurkat cell lysates were treated with peroxynitrite, the YF motif tyrosine of Prx1 was identified as nitrated (47).

Prx are key enzymes for detoxifying H_2O_2 as well as sensing H_2O_2 in redox signaling. In this context, the modulation of Prx peroxidase activity and interaction with other proteins is critical. Modification of the reactive cysteine causes inactivation of the peroxidase activity as seen for overoxidation to sulfinic/sulfonic acid. Glutathionylation and *S*-nitrosation of C_P have also been reported (48–50). Interestingly, phosphorylation of noncatalytic residues in Prx1 and Prx2 could decrease, as well as increase, their peroxidase activity, suggesting a fine interplay between H_2O_2- and kinase-driven signaling pathways (51–54). Similar to our results, *N*-acetylation of Lys-196 in Prx2 causes an increase in peroxidase activity and a decrease in overoxidation susceptibility (55). Again, modification of residues at the C terminus, adjacent to C_R (Lys-196, Thr-194, and Tyr-193 in this work) can affect activity and the extent of overoxidation.

Nitration of tyrosine residues has an impact on protein structure and activity (in general, inactivation, although a gain of function has also been reported) and is linked to a variety of pathological conditions such as neurodegenerative and cardiovascular diseases (56, 57). Nitration of typical 2-Cys Prx has been reported *in vitro* and *in vivo* (20, 47, 58). In particular, Prx2 was identified in a proteomic analysis as one of the nitrated brain proteins in early Alzheimer disease (20). This could have an impact on intracellular H_2O_2-induced signaling cascades, including Prx2-protein interactions, which still remains to be explored. Our work characterizes the nitrated form of Prx2 as a more active and robust peroxidase by favoring the intermolecular disulfide formation, placing tyrosine nitration as another mechanism of modulating Prx in the complex network of redox signaling.

Acknowledgments—We thank M. P. Samuel, M. J. Thomas, and K. J. Nelson (Wake Forest School of Medicine, Winston-Salem, NC) for assistance in samples preparation and whole protein mass spectrometry analysis; B. Alvarez and G. Ferrer-Sueta (Universidad de la República, UdelaR, Uruguay) for helpful discussions; J. Santos (Universidad de Buenos Aires, Argentina) for kindly providing EcTrx1 plasmid; G. Salinas (Institut Pasteur de Montevideo, Uruguay) for the EgTR protein; and L. Blixen for graphical work assistance.

REFERENCES

1. Rhee, S. G., Chae, H. Z., and Kim, K. (2005) Peroxiredoxins: a historical overview and speculative preview of novel mechanisms and emerging concepts in cell signaling. *Free Radic. Biol. Med.* **38,** 1543–1552
2. Wood, Z. A., Poole, L. B., and Karplus, P. A. (2003) Peroxiredoxin evolution and the regulation of hydrogen peroxide signaling. *Science* **300,** 650–653
3. Wood, Z. A., Schröder, E., Robin Harris, J., and Poole, L. B. (2003) Structure, mechanism and regulation of peroxiredoxins. *Trends Biochem. Sci.* **28,** 32–40

4. Hofmann, B., Hecht, H. J., and Flohé, L. (2002) Peroxiredoxins. *Biol. Chem.* **383,** 347–364
5. Copley, S. D., Novak, W. R., and Babbitt, P. C. (2004) Divergence of function in the thioredoxin fold suprafamily: evidence for evolution of peroxiredoxins from a thioredoxin-like ancestor. *Biochemistry* **43,** 13981–13995
6. Schröder, E., Littlechild, J. A., Lebedev, A. A., Errington, N., Vagin, A. A., and Isupov, M. N. (2000) Crystal structure of decameric 2-Cys peroxiredoxin from human erythrocytes at 1.7 Å resolution. *Structure* **8,** 605–615
7. Wood, Z. A., Poole, L. B., Hantgan, R. R., and Karplus, P. A. (2002) Dimers to doughnuts: redox-sensitive oligomerization of 2-cysteine peroxiredoxins. *Biochemistry* **41,** 5493–5504
8. Perkins, A., Nelson, K. J., Williams, J. R., Parsonage, D., Poole, L. B., and Karplus, P. A. (2013) The sensitive balance between fully folded and locally unfolded conformations of a model peroxiredoxin. *Biochemistry* **52,** 8708–8721
9. Biteau, B., Labarre, J., and Toledano, M. B. (2003) ATP-dependent reduction of cysteine-sulphinic acid by *S. cerevisiae* sulphiredoxin. *Nature* **425,** 980–984
10. Jönsson, T. J., Murray, M. S., Johnson, L. C., and Lowther, W. T. (2008) Reduction of cysteine sulfinic acid in peroxiredoxin by sulfiredoxin proceeds directly through a sulfinic phosphoryl ester intermediate. *J. Biol. Chem.* **283,** 23846–23851
11. Winterbourn, C. C., and Hampton, M. B. (2008) Thiol chemistry and specificity in redox signaling. *Free Radic. Biol. Med.* **45,** 549–561
12. Flohé, L., and Ursini, F. (2008) Peroxidase: a term of many meanings. *Antioxid. Redox Signal.* **10,** 1485–1490
13. Ferrer-Sueta, G., Manta, B., Botti, H., Radi, R., Trujillo, M., and Denicola, A. (2011) Factors affecting protein thiol reactivity and specificity in peroxide reduction. *Chem. Res. Toxicol.* **24,** 434–450
14. Randall, L. M., Ferrer-Sueta, G., and Denicola, A. (2013) Peroxiredoxins as preferential targets in H_2O_2-induced signaling. *Methods Enzymol.* **527,** 41–63
15. Sobotta, M. C., Barata, A. G., Schmidt, U., Mueller, S., Millonig, G., and Dick, T. P. (2013) Exposing cells to H_2O_2: a quantitative comparison between continuous low-dose and one-time high-dose treatments. *Free Radic. Biol. Med.* **60,** 325–335
16. Lowther, W. T, and Haynes, A. C. (2011) Reduction of cysteine sulfinic acid in eukaryotic, typical 2-Cys peroxiredoxins by sulfiredoxin. *Antioxid. Redox Signal.* **15,** 99–109
17. Moore, R. B., Mankad, M. V., Shriver, S. K., Mankad, V. N., and Plishker, G. A. (1991) Reconstitution of Ca^{2+}-dependent K^+ transport in erythrocyte membrane vesicles requires a cytoplasmic protein. *J. Biol. Chem.* **266,** 18964–18968
18. Cho, C. S., Kato, G. J., Yang, S. H., Bae, S. W., Lee, J. S., Gladwin, M. T., and Rhee, S. G. (2010) Hydroxyurea-induced expression of glutathione peroxidase 1 in red blood cells of individuals with sickle cell anemia. *Antioxid. Redox Signal.* **13,** 1–11
19. Manta, B., Hugo, M., Ortiz, C., Ferrer-Sueta, G., Trujillo, M., and Denicola, A. (2009) The peroxidase and peroxynitrite reductase activity of human erythrocyte peroxiredoxin 2. *Arch. Biochem. Biophys.* **484,** 146–154
20. Reed, T. T., Pierce, W. M., Jr., Turner, D. M., Markesbery, W. R., and Butterfield, D. A. (2009) Proteomic identification of nitrated brain proteins in early Alzheimer's disease inferior parietal lobule. *J. Cell. Mol. Med.* **13,** 2019–2029
21. Denicola, A., Alvarez, B., and Thomson, L. (2008) *Free Radical Pathophysiology* (Alvarez, S. and Evelson, P., eds) pp. 39–55, Transworld Research Network, India
22. Radi, R. (2004) Nitric oxide, oxidants, and protein tyrosine nitration. *Proc. Natl. Acad. Sci. U.S.A.* **101,** 4003–4008
23. Trujillo, M., Ferrer-Sueta, G., and Radi, R. (2008) Peroxynitrite detoxification and its biologic implications. *Antioxid. Redox Signal.* **10,** 1607–1620
24. Trujillo, M., Alvarez, B., Souza, J. M., Romero, N., Castro, L., Thomson, L., and Radi, R. (2010) *Nitric Oxide Biology and Pathobiology* (Ignarro, L. J., ed) pp. 61–102, Academic Press, Orlando, FL
25. Beckman, J. S., Beckman, T. W., Chen, J., Marshall, P. A., and Freeman, B. A. (1990) Apparent hydroxyl radical production by peroxynitrite: implications for endothelial injury from nitric oxide and superoxide. *Proc. Natl. Acad. Sci. U.S.A.* **87,** 1620–1624
26. Romero, N., Radi, R., Linares, E., Augusto, O., Detweiler, C. D., Mason, R. P., and Denicola, A. (2003) Reaction of human hemoglobin with peroxynitrite: isomerization to nitrate and secondary formation of protein radicals. *J. Biol. Chem.* **278,** 44049–44057
27. Poole, L. B., Godzik, A., Nayeem, A., and Schmitt, J. D. (2000) AhpF can be dissected into two functional units: tandem repeats of two thioredoxin-like folds in the N-terminus mediate electron transfer from the thioredoxin reductase-like C-terminus to AhpC. *Biochemistry* **39,** 6602–6615
28. Bonilla, M., Denicola, A., Marino, S. M., Gladyshev, V. N., and Salinas, G. (2011) Linked thioredoxin-glutathione systems in platyhelminth parasites: alternative pathways for glutathione reduction and deglutathionylation. *J. Biol. Chem.* **286,** 4959–4967
29. Pace, C. N., Vajdos, F., Fee, L., Grimsley, G., and Gray, T. (1995) How to measure and predict the molar absorption coefficient of a protein. *Protein Sci.* **4,** 2411–2423
30. Egwim, I. O., and Gruber, H. J. (2001) Spectrophotometric measurement of mercaptans with 4,4′-dithiodipyridine. *Anal. Biochem.* **288,** 188–194
31. Brito, C., Naviliat, M., Tiscornia, A. C., Vuillier, F., Gualco, G., Dighiero, G., Radi, R., and Cayota, A. M. (1999) Peroxynitrite inhibits T lymphocyte activation and proliferation by promoting impairment of tyrosine phosphorylation and peroxynitrite-driven apoptotic death. *J. Immunol.* **162,** 3356–3366
32. Jörnvall, H., and Jollès, P. (2000) Protein structure analysis of today: proteomics in functional genomics. *EXS* **88,** XI–XIII
33. Peskin, A. V., Dickerhof, N., Poynton, R. A., Paton, L. N., Pace, P. E., Hampton, M. B., and Winterbourn, C. C. (2013) Hyperoxidation of peroxiredoxins 2 and 3: rate constants for the reactions of the sulfenic acid of the peroxidatic cysteine. *J. Biol. Chem.* **288,** 14170–14177
34. Nelson, K. J., Parsonage, D., Karplus, P. A., and Poole, L. B. (2013) Evaluating peroxiredoxin sensitivity toward inactivation by peroxide substrates. *Methods Enzymol.* **527,** 21–40
35. Haynes, A. C., Qian, J., Reisz, J. A., Furdui, C. M., and Lowther, W. T. (2013) Molecular basis for the resistance of human mitochondrial 2-Cys peroxiredoxin 3 to hyperoxidation. *J. Biol. Chem.* **288,** 29714–29723
36. Yuan, Y., Knaggs, M., Poole, L., Fetrow, J., and Salsbury, F., Jr. (2010) Conformational and oligomeric effects on the cysteine pK_a of tryparedoxin peroxidase. *J. Biomol. Struct. Dyn.* **28,** 51–70
37. Salsbury, F. R., Jr., Yuan, Y., Knaggs, M. H., Poole, L. B., and Fetrow, J. S. (2012) Structural and electrostatic asymmetry at the active site in typical and atypical peroxiredoxin dimers. *J. Phys. Chem. B* **116,** 6832–6843
38. Budde, H., Flohé, L., Hecht, H. J., Hofmann, B., Stehr, M., Wissing, J., and Lünsdorf, H. (2003) Kinetics and redox-sensitive oligomerisation reveal negative subunit cooperativity in tryparedoxin peroxidase of *Trypanosoma brucei brucei*. *Biol. Chem.* **384,** 619–633
39. Peskin, A. V., Low, F. M., Paton, L. N., Maghzal, G. J., Hampton, M. B., and Winterbourn, C. C. (2007) The high reactivity of peroxiredoxin 2 with H_2O_2 is not reflected in its reaction with other oxidants and thiol reagents. *J. Biol. Chem.* **282,** 11885–11892
40. Fomenko, D. E., Koc, A., Agisheva, N., Jacobsen, M., Kaya, A., Malinouski, M., Rutherford, J. C., Siu, K. L., Jin, D. Y., Winge, D. R., and Gladyshev, V. N. (2011) Thiol peroxidases mediate specific genome-wide regulation of gene expression in response to hydrogen peroxide. *Proc. Natl. Acad. Sci. U.S.A.* **108,** 2729–2734
41. Oláhová, M, Taylor, S. R., Khazaipoul, S., Wang, J., Morgan, B. A., Matsumoto, K., Blackwell, T. K., and Veal, E. A. (2008) A redox-sensitive peroxiredoxin that is important for longevity has tissue- and stress-specific roles in stress resistance. *Proc. Natl. Acad. Sci. U.S.A.* **105,** 19839–19844
42. Day, A. M., Brown, J. D., Taylor, S. R., Rand, J. D., Morgan, B. A., and Veal, E. A. (2012) Inactivation of a peroxiredoxin by hydrogen peroxide is critical for thioredoxin-mediated repair of oxidized proteins and cell survival. *Mol. Cell* **45,** 398–408
43. Veal, E. A., Day, A. M., and Morgan, B. A. (2007) Hydrogen peroxide sensing and signaling. *Mol. Cell* **26,** 1–14
44. Rhee, S. G. (2006) Cell signaling: H_2O_2, a necessary evil for cell signaling. *Science* **312,** 1882–1883
45. Koo, K. H., Lee, S., Jeong, S. Y., Kim, E. T., Kim, H. J., Kim, K., Song, K., and Chae, H. Z. (2002) Regulation of thioredoxin peroxidase activity by C-ter-

minal truncation. *Arch. Biochem. Biophys.* **397,** 312–318
46. Sayed, A. A., and Williams, D. L. (2004) Biochemical characterization of 2-Cys peroxiredoxins from *Schistosoma mansoni*. *J. Biol. Chem.* **279,** 26159–26166
47. Ghesquière, B., Colaert, N., Helsens, K., Dejager, L., Vanhaute, C., Verleysen, K., Kas, K., Timmerman, E., Goethals, M., Libert, C., Vandekerckhove, J., and Gevaert, K. (2009) *In vitro* and *in vivo* protein-bound tyrosine nitration characterized by diagonal chromatography. *Mol. Cell. Proteomics* **8,** 2642–2652
48. Park, J. W., Piszczek, G., Rhee, S. G., and Chock, P. B. (2011) Glutathionylation of peroxiredoxin I induces decamer to dimers dissociation with concomitant loss of chaperone activity. *Biochemistry* **50,** 3204–3210
49. Fang, J., Nakamura, T., Cho, D. H., Gu, Z., and Lipton, S. A. (2007) *S*-Nitrosylation of peroxiredoxin 2 promotes oxidative stress-induced neuronal cell death in Parkinson's disease. *Proc. Natl. Acad. Sci. U.S.A.* **104,** 18742–18747
50. Engelman, R., Weisman-Shomer, P., Ziv, T., Xu, J., Arnér, E. S., and Benhar, M. (2013) Multilevel regulation of 2-Cys peroxiredoxin reaction cycle by *S*-nitrosylation. *J. Biol. Chem.* **288,** 11312–11324
51. Jang, H. H., Kim, S. Y., Park, S. K., Jeon, H. S., Lee, Y. M., Jung, J. H., Lee, S. Y., Chae, H. B., Jung, Y. J., Lee, K. O., Lim, C. O., Chung, W. S., Bahk, J. D., Yun, D. J., Cho, M. J., and Lee, S. Y. (2006) Phosphorylation and concomitant structural changes in human 2-Cys peroxiredoxin isotype I differentially regulate its peroxidase and molecular chaperone functions. *FEBS Lett.* **580,** 351–355
52. Woo, H. A., Yim, S. H., Shin, D. H., Kang, D., Yu, D. Y., and Rhee, S. G. (2010) Inactivation of peroxiredoxin I by phosphorylation allows localized H_2O_2 accumulation for cell signaling. *Cell* **140,** 517–528
53. Zykova, T. A., Zhu, F., Vakorina, T. I., Zhang, J., Higgins, L. A., Urusova, D. V., Bode, A. M., and Dong, Z. (2010) T-LAK cell-originated protein kinase (TOPK) phosphorylation of Prx1 at Ser-32 prevents UVB-induced apoptosis in RPMI7951 melanoma cells through the regulation of Prx1 peroxidase activity. *J. Biol. Chem.* **285,** 29138–29146
54. Chang, T. S., Jeong, W., Choi, S. Y., Yu, S., Kang, S. W., and Rhee, S. G. (2002) Regulation of peroxiredoxin I activity by Cdc2-mediated phosphorylation. *J. Biol. Chem.* **277,** 25370–25376
55. Parmigiani, R. B., Xu, W. S., Venta-Perez, G., Erdjument-Bromage, H., Yaneva, M., Tempst, P., and Marks, P. A. (2008) HDAC6 is a specific deacetylase of peroxiredoxins and is involved in redox regulation. *Proc. Natl. Acad. Sci. U.S.A.* **105,** 9633–9638
56. Perry, G., Raina, A. K., Nunomura, A., Wataya, T., Sayre, L. M., and Smith, M. A. (2000) How important is oxidative damage? Lessons from Alzheimer's disease. *Free Radic. Biol. Med.* **28,** 831–834
57. Leite, P. F., Liberman, M., Sandoli de Brito, F., and Laurindo, F. R. (2004) Redox processes underlying the vascular repair reaction. *World J. Surg.* **28,** 331–336
58. Turko, I. V., Li, L., Aulak, K. S., Stuehr, D. J., Chang, J. Y., and Murad, F. (2003) Protein tyrosine nitration in the mitochondria from diabetic mouse heart: implications to dysfunctional mitochondria in diabetes. *J. Biol. Chem.* **278,** 33972–33977